



UNIVERSITY
OF ALBERTA

State-Delays in Chemical Engineering: A Control Framework for Distributed Parameter Systems

Behrad 'Brad' Moadeli

Department of Chemical and Materials Engineering, University of Alberta
Edmonton, Alberta, Canada

September 5th, 2025

Distributed Parameter Systems in Chemical Engineering

- Chemical processes \rightarrow PDEs \rightarrow **Distributed Parameter Systems (DPSs)**.
- A canonical example \rightarrow **Axial-Dispersion Tubular Reactors** \rightarrow 2nd order Parabolic PDEs.
- Common in practice \rightarrow **Recycle Streams** \rightarrow Alter system dynamics. (Khatibi et al., 2021)

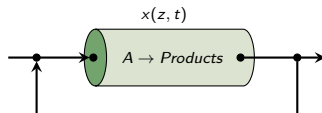


Figure: Axial tubular reactor with recycle stream.

Governing equation, general form

$$\partial_t x(\zeta, t) = \begin{aligned} & D \partial_\zeta^2 x(\zeta, t) && \text{Dispersion} \\ & -v \partial_\zeta x(\zeta, t) && \text{Convection} \\ & -k x(\zeta, t) && \text{Reaction} \end{aligned} \quad (1)$$

Early Lumping vs. Late Lumping

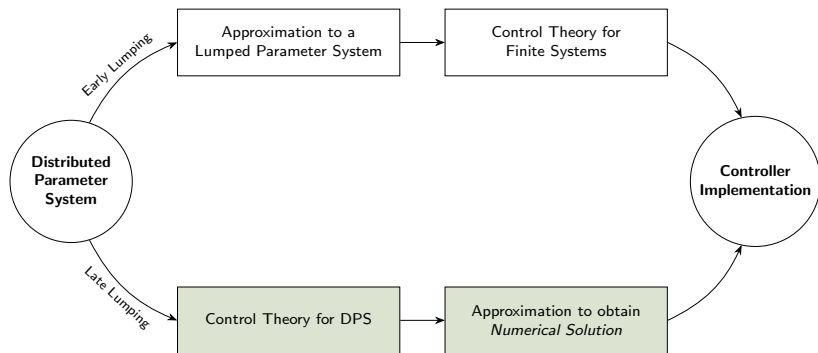


Figure: Conceptual comparison between early and late lumping control strategies. (Cassol, 2022)

Motivation: What's Missing?

Prior Work:

- Late lumping → well-developed for DPS control. (Curtain and Zwart, 2020; Christofides, 2012)
- Control of Parabolic PDEs → well-developed → e.g., Reactors w/o recycle. (Liu et al., 2014; Xu and Dubljevic, 2017)
- Reactors with recycle studied (Khatibi et al., 2021) → Instantaneous recycle

The Gap:

- Reality: Recycle takes time to travel.
- This travel time → **State Delay**.
- Unlike actuation/measurement delays → Absent in ChemEng DPS literature.
- No control framework to capture state delays in ChemEng DPS.

End Goal

To develop a **modeling and control framework** via **late-lumping** approach, for chemical engineering **DPSs with state delays**, by studying axial dispersion tubular reactors as a *general yet practically relevant* case.

Recycle-Induced State Delay: A Closer Look

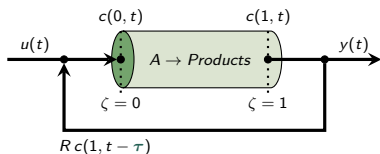


Figure: Axial tubular reactor with recycle-induced state delay.

General Setup:

- 2nd order parabolic PDE.
- Danckwerts-type boundary conditions.

Governing PDE (Isothermal)

$$\begin{aligned} \partial_t c(\zeta, t) &= D \partial_\zeta^2 c(\zeta, t) - v \partial_\zeta c(\zeta, t) - k_r c(\zeta, t) \\ \begin{cases} D \partial_\zeta c(0, t) - v c(0, t) = -v [R c(1, t - \tau) + (1 - R) u(t)] \\ \partial_\zeta c(1, t) = 0 \\ y(t) = c(1, t) \end{cases} \end{aligned} \quad (2)$$

Key Novelty: Delay as a Transport PDE

- A transport PDE over $\zeta \in [0, 1]$:

$$\frac{\partial x}{\partial t} - \frac{1}{\tau} \frac{\partial x}{\partial \zeta} = 0, \quad x(0, t) = u(t)$$

- Describes propagation of input $u(t)$ with delay:

$$x(1, t) = u(t - \tau)$$

- Delay emerges as **residence time** across domain.
- Foundation for modeling **state delay** as a PDE. (Krstić, 2009)

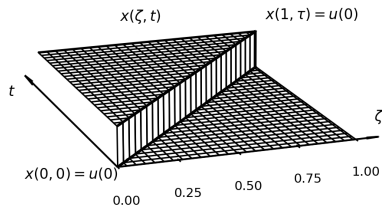


Figure: A step input propagates spatially and appears at the outlet with delay τ .

Coupled PDE System

Results in a **time-invariant** representation of the system, suitable for **infinite-dimensional control theory**.

Overall Trajectory

Table: Thesis trajectory across Chapters 2–4.

Thesis chapter	Model assumption	Temporal domain	Controller strategy	Estimation method	Publications
Chapter 2	Isothermal	Continuous-time	LQR (unconstrained)	Luenberger observer (unconstrained)	(Moadeli et al., 2025)
Chapter 3	Isothermal	Discrete-time	MPC (constrained)	Luenberger observer (unconstrained)	(Moadeli and Dubljevic, 2025b,c)
Chapter 4	Non-isothermal	Discrete-time	MPC (constrained)	MHE (constrained)	(Moadeli and Dubljevic, 2025a)

Chapter 2: Continuous-time Estimation and Optimal Control for the Isothermal System

Table: Thesis trajectory across Chapters 2–4.

Thesis chapter	Model assumption	Temporal domain	Controller strategy	Estimation method	Publications
Chapter 2	Isothermal	Continuous-time	LQR (unconstrained)	Luenberger observer (unconstrained)	(Moadeli et al., 2025)
Chapter 3	Isothermal	Discrete-time	MPC (constrained)	Luenberger observer (unconstrained)	(Moadeli and Dubljevic, 2025b,c)
Chapter 4	Non-isothermal	Discrete-time	MPC (constrained)	MHE (constrained)	(Moadeli and Dubljevic, 2025a)

Infinite-Dimensional State-Space Representation

System Dynamics

$$\dot{x}(\zeta, t) = Ax(\zeta, t) + Bu(t); \quad y(t) = Cx(\zeta, t) \quad (3)$$

$$A := \begin{bmatrix} D\partial_{\zeta\zeta} - v\partial_{\zeta} - k_r & 0 \\ 0 & \frac{1}{\tau}\partial_{\zeta} \end{bmatrix}$$

$$x := \begin{bmatrix} x_1 \\ x_2 \end{bmatrix} \in L^2[0, 1] \times L^2[0, 1]$$

$$\begin{aligned} \mathcal{D}(A) = \left\{ x(\zeta) = [x_1(\zeta), x_2(\zeta)]^T \in X : \right. \\ x(\zeta), \partial_{\zeta}x(\zeta), \partial_{\zeta\zeta}x(\zeta) \quad \text{a.c.}, \\ D\partial_{\zeta}x_1(0) - vx_1(0) = -vRx_2(0), \\ \left. \partial_{\zeta}x_1(1) = 0, x_1(1) = x_2(1) \right\} \end{aligned} \quad (4)$$

$$B := \begin{bmatrix} \delta(\zeta) \\ 0 \end{bmatrix} v(1 - R) \quad (5)$$

$$C := \begin{bmatrix} \int_0^1 \delta(\zeta - 1)(\cdot) d\zeta & 0 \end{bmatrix}$$

$$D = 0$$

Eigenvalue Distribution: System is Unstable

- Spectrum of system generator $\sigma(A)$ determines open-loop stability.
- Characteristics equation $\det(\lambda_i - A) = 0$ is solved to obtain eigenvalues.
- Direct analytical solution is impractical—solved numerically.
- Result: eigenvalues with **positive real parts** \rightarrow **open-loop unstable**.
- Parameters used to obtain the eigenvalue distribution are given in Table 7 in Appendix.

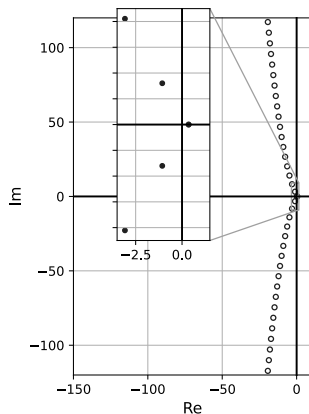


Figure: Eigenvalue distribution of system operator A

LQR: Operator Riccati Equation

■ Cost:

$$J = \int_0^\infty \langle x, Qx \rangle + \langle u, Ru \rangle ds.$$

- Solve operator Riccati for Π ;
truncate in biorthogonal basis to
get matrix Riccati for $P = [p_{ij}]$.

$$u(t) = -\langle k_{\text{ric}}(\zeta), x(\zeta, t) \rangle = -B^* \Pi x(\zeta, t),$$

$$k_{\text{ric}}(\zeta) \equiv \sum_{i=1}^N \sum_{j=1}^N p_{i,j} \gamma_i \bar{\psi}_j(\zeta)$$

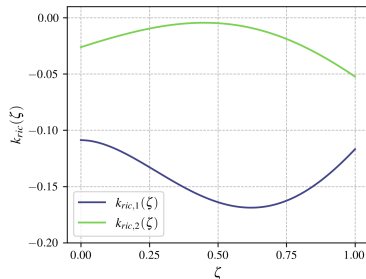


Figure: $k_{\text{ric}}(\zeta)$, $N=3$

Observer Design and Pole Placement

- Output operator (point measurement): $C = \left[\int_0^1 \delta(\zeta - 1)(\cdot) d\zeta, 0 \right]$.
- Choose $L(\zeta)$ s.t. $A - LC$ has desired eigenvalues (to the left of regulator poles).
- Error dynamics: $\dot{e} = (A - LC)e$.

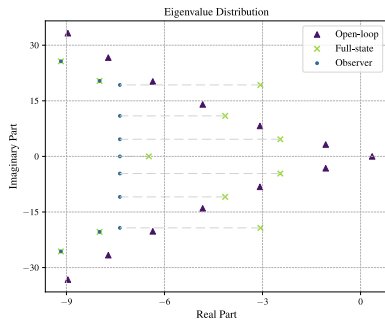
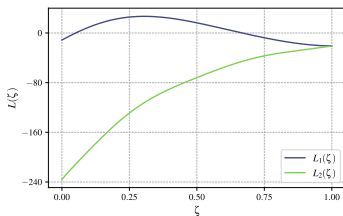


Figure: Observer gain profile and closed-loop eigenvalue placement.

Results: Stabilization Achieved (FDM validation)

- Both full-state LQR and observer-based output feedback stabilize the PDE system (finite-difference validation).
- Observer-based loop is slightly more sluggish but robust and stable.
- Delay sensitivity: maintains stability for moderate τ mismatch used in design.

State Profile under Observer-based Feedback $x_1(\zeta, t)$

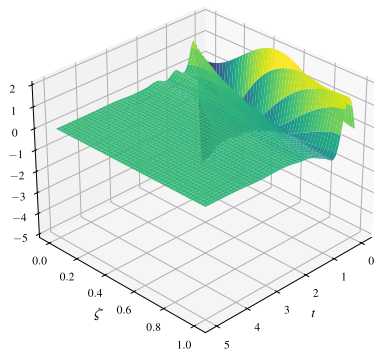


Figure: Closed-loop $x_1(\zeta, t)$ (LQR)

Chapter 3: Discrete-time Estimation and Model Predictive Control for the Isothermal System

Table: Thesis trajectory across Chapters 2–4.

Thesis chapter	Model assumption	Temporal domain	Controller strategy	Estimation method	Publications
Chapter 2	Isothermal	Continuous-time	LQR (unconstrained)	Luenberger observer (unconstrained)	(Moadeli et al., 2025)
Chapter 3	Isothermal	Discrete-time	MPC (constrained)	Luenberger observer (unconstrained)	(Moadeli and Dubljevic, 2025b,c)
Chapter 4	Non-isothermal	Discrete-time	MPC (constrained)	MHE (constrained)	(Moadeli and Dubljevic, 2025a)

Cayley-Tustin Time-Discretization

Discrete-time System

$$\begin{aligned}\dot{x}(\zeta, k) &= A_d x(\zeta, k-1) + B_d u(k) \\ y(k) &= C_d x(\zeta, k-1) + D_d u(k)\end{aligned}\quad (6)$$

- Discretization is needed for **digital controller implementation**.
- Cayley-Tustin discretization preserves:
 - System's **infinite-dimensional structure**
 - **Stability** and **controllability**
 - ...

continuous- to discrete-time mapping

$$\begin{aligned}A_d &= -I + 2\alpha R(\alpha, A), \\ B_d &= \sqrt{2\alpha} R(\alpha, A) B, \\ C_d &= \sqrt{2\alpha} C R(\alpha, A), \\ D_d &= C R(\alpha, A) B\end{aligned}\quad (7)$$

- $R(\alpha, A) := [\alpha I - A]^{-1}$ is the **resolvent operator** of system generator A .
- $\alpha = \frac{2}{\Delta t}$, where Δt is the sampling time.

Resolvent Operator: Role and Procedure

- To follow the **late-lumping** approach, it is crucial to obtain a **closed-form representation** of the resolvent operator, which bridges the continuous- and discrete-time domains.
- This is done by interpreting the resolvent as a **mapping** from either *initial conditions* or *inputs* to the *Laplace-transformed state*.

Laplace Transform

$$\begin{aligned} \dot{x}(\zeta, t) &= Ax(\zeta, t) + Bu(t) \xrightarrow{\mathcal{L}} \\ sx(\zeta, s) - x(\zeta, 0) &= Ax(\zeta, s) + BU(s) \\ \begin{cases} u = 0 \rightarrow x = R(s, A)x(0) \\ x(0) = 0 \rightarrow x = R(s, A)BU(s) \end{cases} \end{aligned} \quad (8)$$

To compute $R(s, A)$:

- Apply Laplace transform to the PDE system.
- Reformulate as a spatial ODE in ζ , solve using $e^{P(s)\zeta}$.
- Enforce boundary conditions to determine $\tilde{X}(0, s)$.
- Combine terms to obtain closed-form $R(s, A)$.

See slide 38 in Appendix for full derivation

Continuous-Time Luenberger Observer Design

- State measurements in DPSs are infeasible: states are distributed over space. A **Luenberger observer** reconstructs full state using output $y(t)$.

- Observer dynamics:

$$\begin{aligned}\dot{\hat{x}}(\zeta, t) &= A\hat{x}(\zeta, t) + Bu(t) \\ &\quad + L_c [y(t) - \hat{y}(t)], \\ \hat{y}(t) &= C\hat{x}(\zeta, t)\end{aligned}\quad (9)$$

- Estimation error:

$e(\zeta, t) = x(\zeta, t) - \hat{x}(\zeta, t)$, evolves as $\dot{e}(\zeta, t) = (A - L_c C)e(\zeta, t) = A_o e(\zeta, t)$.

- Gain $L_c = f(\zeta, l_{obs})$ is tuned to place A_o eigenvalues in left half-plane.

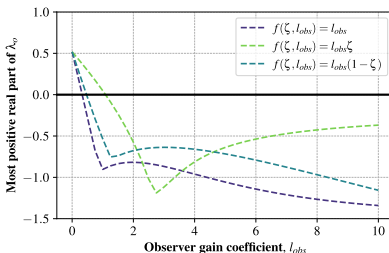


Figure: The effect of various observer gains $L_c = f(\zeta, l_{obs})$ on the eigenvalues of state reconstruction error dynamics λ_o .

Discrete-Time Observer via Cayley-Tustin

- Cayley-Tustin time discretization yields a DT observer in the form:

$$\begin{aligned}\hat{x}(\zeta, k) &= A_d \hat{x}(\zeta, k-1) + B_d u(k) + L_d [y(k) - \hat{y}(k)] \\ \hat{y}(k) &= C_{d,o} \hat{x}(\zeta, k-1) + D_{d,o} u(k) + M_{d,o} y(k)\end{aligned}\tag{10}$$

- with the following continuous- to discrete-time mapping:

$$\begin{aligned}C_{d,o}(\cdot) &= \sqrt{2\alpha} [I + C(\alpha I - A)L_c]^{-1} CR(\alpha, A)(\cdot) \\ D_{d,o} &= [I + C(\alpha I - A)L_c]^{-1} CR(\alpha, A)B \\ M_{d,o} &= [I + CR(\alpha, A)L_c]^{-1} CR(\alpha, A)L_c \\ L_d &= \sqrt{2\alpha} R(\alpha, A)L_c\end{aligned}\tag{11}$$

- Resulting DT error dynamics are stable **if CT observer is stable** (Xu and Dubljevic, 2016).

Key Point

No spatial discretization: Observer is constructed using the same resolvent operator.

MPC Architecture: Output-Feedback Loop

- Observer reconstructs $\hat{x}(k)$, passed to MPC at each time step.
- MPC uses predicted future states and solves constrained QP over a finite horizon.
- Only the first control input is applied → **receding horizon**.

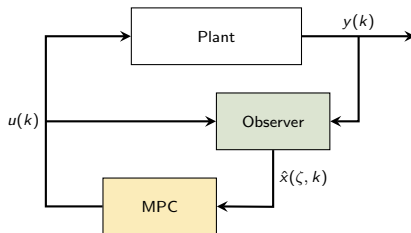


Figure: Block diagram representation of the observer-based MPC.

MPC Formulation with Terminal Projection

■ Finite-horizon MPC:

$$\min_U \sum_{l=0}^{N-1} \langle \hat{x}(\zeta, k+l|k), Q\hat{x}(\zeta, k+l|k) \rangle \\ + \langle u(k+l+1|k), Fu(k+l+1|k) \rangle \\ + \langle \hat{x}(\zeta, k+N|k), P\hat{x}(\zeta, k+N|k) \rangle$$

$$\text{s.t. } \hat{x}(\zeta, k+l|k) = \\ A_d \hat{x}(\zeta, k+l-1|k) + B_d u(k+l|k) \\ u^{\min} \leq u(k+l|k) \leq u^{\max} \\ \langle \hat{x}(\zeta, k+N|k), \phi_u(\zeta) \rangle = 0 \quad (12)$$

- P is the **terminal cost operator** obtained as the solution to the *discrete-time Lyapunov* equation:

$$P(\cdot) = \sum_{m=0}^{\infty} \sum_{n=0}^{\infty} -\frac{\langle \phi_m, Q\psi_n \rangle}{\lambda_m + \bar{\lambda}_n} \langle (\cdot), \psi_n \rangle \phi_m \quad (13)$$

- The constrained QP is **convex** only if P is **positive definite**.
- P is positive definite only if the terminal state $\hat{x}(\zeta, k+N|k)$ is in a **stable subspace**.
- A **terminal constraint** is introduced as an *equality constraint* by setting the **projection of the terminal state** onto the **unstable subspace** of the system equal to zero.

Results: Stabilization under Observer-based MPC

- Initial condition:
 $x_1(\zeta, 0) = \sin^2(\pi\zeta)$, $x_2(\zeta, 0) = 0$
- Sampling time $\Delta t = 20$ s
- Horizon length $N = 9$
- Input bounds: $0 \leq u(t) \leq 0.15$

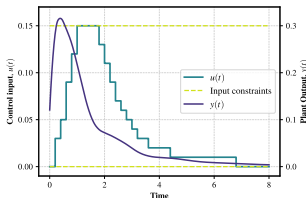


Figure: Control input and reactor output under MPC.

Observer-based MPC State Response

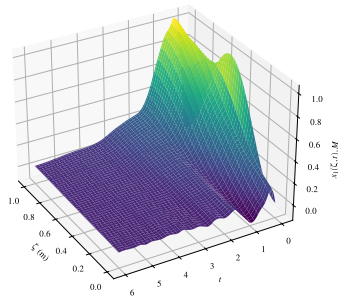


Figure: Stabilized concentration profile under observer-MPC.

Chapter 4: Non-isothermal System—Moving Horizon Estimation and Model Predictive Control

Table: Thesis trajectory across Chapters 2–4.

Thesis chapter	Model assumption	Temporal domain	Controller strategy	Estimation method	Publications
Chapter 2	Isothermal	Continuous-time	LQR (unconstrained)	Luenberger observer (unconstrained)	(Moadeli et al., 2025)
Chapter 3	Isothermal	Discrete-time	MPC (constrained)	Luenberger observer (unconstrained)	(Moadeli and Dubljevic, 2025b,c)
Chapter 4	Non-isothermal	Discrete-time	MPC (constrained)	MHE (constrained)	(Moadeli and Dubljevic, 2025a)

Non-isothermal System Model

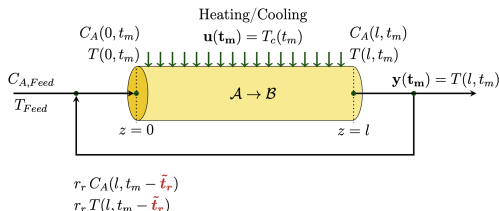


Figure: Non-isothermal system schematic.

States: $x = [m_1(\zeta, t), m_2(\zeta, t), m_3(\zeta, t), m_4(\zeta, t)]^T$ (reactor concentration/temperature and their recycle-line counterparts).

Input: wall/jacket temperature $u(t) = T_w(t)$. **Output:** $y(t) = m_2(1, t)$ (outlet temperature).

$$\partial_t m_1 = \frac{1}{Pe_m} \partial_{\zeta\zeta} m_1 - \partial_{\zeta} m_1 + k_a(1 - m_1) e^{\frac{\eta m_2}{1+m_2}},$$

$$\partial_t m_2 = \frac{1}{Pe_T} \partial_{\zeta\zeta} m_2 - \partial_{\zeta} m_2 + \alpha k_a(1 - m_1) e^{\frac{\eta m_2}{1+m_2}} + \sigma(T_w(t) - m_2),$$

$$\partial_t m_3 = \frac{1}{\tau} \partial_{\zeta} m_3, \quad \partial_t m_4 = \frac{1}{\tau} \partial_{\zeta} m_4,$$

with recycle boundary coupling and Danckwerts boundary conditions.

Linearized, Dimensionless Representation of the Non-linear System around Steady States

System Dynamics

$$\dot{x}(\zeta, t) = Ax(\zeta, t) + Bu(t); \quad y(t) = Cx(\zeta, t) \quad (14)$$

- Dimensionless Model
- Steady-State Analysis
- Deviation Variables
- Linearization

$$\mathfrak{B}(\cdot) = \begin{bmatrix} 0 \\ \sigma \\ 0 \\ 0 \end{bmatrix} (\cdot) \quad (15)$$

$$\mathfrak{C}(\cdot) = \begin{bmatrix} 0 & \int_0^1 \delta(\zeta - 1)(\cdot)_2 d\zeta & 0 & 0 \end{bmatrix} \quad (16)$$

Linearized, Dimensionless Representation of the Non-linear System around Steady States

$$A(\cdot) = \begin{bmatrix} \frac{1}{Pe_m} \partial_{\zeta\zeta} - \partial_{\zeta} + R_1 & R_2 & 0 & 0 \\ \alpha R_1 & \frac{1}{Pe_T} \partial_{\zeta\zeta} - \partial_{\zeta} + \alpha R_2 - \sigma & 0 & 0 \\ 0 & 0 & \frac{1}{\tau} \partial_{\zeta} & 0 \\ 0 & 0 & 0 & \frac{1}{\tau} \partial_{\zeta} \end{bmatrix} \begin{bmatrix} (\cdot)_1 \\ (\cdot)_2 \\ (\cdot)_3 \\ (\cdot)_4 \end{bmatrix}, \quad (17)$$

$$\begin{aligned} \mathcal{D}(A) := \left\{ x = (x_1, x_2, x_3, x_4)^T \in X : x_1, x_2 \in H^2(0, 1), x_3, x_4 \in H^1(0, 1); \right. \\ \partial_{\zeta} x_1(1) = 0; \quad \partial_{\zeta} x_1(0) = Pe_m [x_1(0) - r_r x_3(0)]; \\ \partial_{\zeta} x_2(1) = 0; \quad \partial_{\zeta} x_2(0) = Pe_T [x_2(0) - r_r x_4(0)]; \\ \left. x_1(1) = x_3(1); \quad x_2(1) = x_4(1) \right\}. \end{aligned} \quad (18)$$

Eigenvalue Distribution: Unstable and Stable Cases

Same as previous chapters, the eigenvalue distribution of the system operator A is analyzed to determine stability, and is obtained by solving the characteristic equation $\det(\lambda_i - A) = 0$. Parameters used to obtain the eigenvalue distributions are given in Table 8 in Appendix.

Eigenvalue Distributions in the Complex Plane

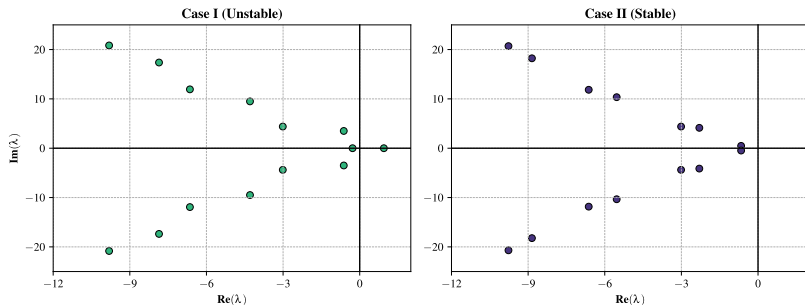


Figure: Eigenvalue distribution in the complex plane for Case I (Unstable) and Case II (Stable).

Moving Horizon Estimation (MHE)

- In distributed parameter systems, full state measurement is not feasible \Rightarrow need an estimator.
- **MHE**: finite-horizon, optimization-based state estimator using most recent N_{MHE} outputs and inputs.
- Model (after Cayley–Tustin discretization of the PDE system):

$$\begin{cases} \hat{x}_{k+1} = \mathfrak{A}_d \hat{x}_k + \mathfrak{B}_d u_k + \mathfrak{N}_d w_k, \\ y_k = \mathfrak{C}_d \hat{x}_k + \mathfrak{D}_d u_k + v_k, \end{cases}$$

where w_k, v_k are process and measurement noise.

- At each step, solve a constrained QP to find the most plausible state and disturbance trajectory consistent with data.
- Naturally handles constraints, disturbances, and produces an estimated state $\hat{x}_{k|k}$ for feedback.
- Discretization in time is Cayley–Tustin (same as in previous chapters); MPC formulation is also the same as before.

MHE-MPC Integration

Table: Proposed MHE-MPC algorithm: Initialization window

-
-
- 0). Assume plant dynamics $\{w_k, v_k\}_{k=0}^{k_{\text{end}}}$ and initial condition x_0 are known. Let $N = N_{\text{MHE}}$.

Initialization window ($T < N$):

- 1). Assign desired values to the input sequence $\{u_k\}_{k=0}^{N-1}$.
- 2). Run the plant model:
$$\left\{ \begin{array}{l} x_{k+1} = \mathfrak{A}_d x_k + \mathfrak{B}_d u_k + \mathfrak{N}_d w_k \\ y_k = \mathfrak{C}_d x_k + \mathfrak{D}_d u_k + v_k \end{array} \right\}_{k=0}^{N-1} \quad \text{to obtain}$$

 $\{y_k\}_{k=0}^{N-1}$.
- 3). Provide an initial guess for $\hat{x}_{0|N-1}$.
-

MHE-MPC Integration

Table: Proposed MHE-MPC algorithm: Control-Estimation window

Control-Estimation window ($T \geq N$):

- 4). Collect $\{u_k, y_k\}_{k=T-N}^{T-1}$ and prior estimate $\hat{x}_{T-N|T-1}$. Solve $\min_{\omega_T} J_{\text{MHE}}$ to obtain $\omega_T = \left[\hat{x}_{T-N|T} \mid \{\hat{w}_k|_T\}_{k=T-N}^{T-1} \right]$
 - 5). Simulate the model: $\{\hat{x}_{k+1|T} = \mathfrak{A}_d \hat{x}_k|_T + \mathfrak{B}_d u_k + \mathfrak{N}_d \hat{w}_k|_T\}_{k=0}^{N-1}$ to compute $\hat{x}_{T-N+1|T}$ and $\hat{x}_{T|T}$.
 - 6). Use $\hat{x}_{T|T}$ to solve $\min_U J_{\text{MPC}}$ and obtain u_T .
 - 7). Apply u_T to the plant:
$$\begin{cases} x_{T+1} &= \mathfrak{A}_d x_T + \mathfrak{B}_d u_T + \mathfrak{N}_d w_T \\ y_T &= \mathfrak{C}_d x_T + \mathfrak{D}_d u_T + v_T \end{cases} \quad \text{to obtain } y_T.$$
 - 8). Update $T \leftarrow T + 1$ and repeat steps 4-8.
-
-

Results: Stabilization under MHE-MPC

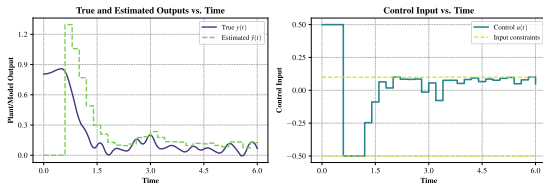


Figure: Case II: output & estimated output over time

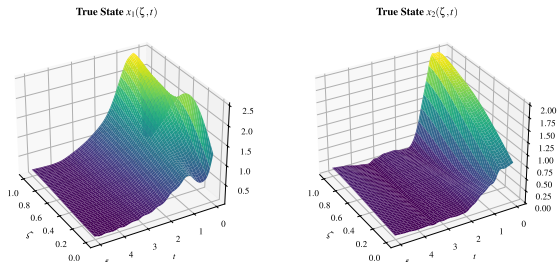


Figure: Case II: stabilization under MHE-MPC

Conclusion — Objectives Achieved

- Revealed **state delay** in chemical engineering DPS
- Utilized a general yet physically meaningful testbed to develop a framework that addresses state delays in chemical engineering DPS via transport PDEs.
- Across studies, controllers **stabilized** otherwise unstable reactor conditions and met key performance criteria, confirming viability of late lumping for delay-affected DPSs.
- Net takeaway: a structure-preserving model + delay-aware estimation/control bring modern methods to practical DPSs with internal delays.

Future Work — Where This Goes Next

- **Robustness & uncertainty:** incorporate model/parametric uncertainty, unmodeled dynamics, time-variation; develop robust/adaptive controllers and observers.
- **Richer objectives:** extend beyond stabilization to setpoint tracking and disturbance rejection within the MPC/regulator designs.
- **Comprehensive delays:** integrate input and output delays alongside state delay using the same transport-PDE framework for more realistic plant-wide behavior.

Thank you!

I'm glad to take your questions.

References

- Cassol, G. O. (2022). *From Continuous Modelling to Discrete Constrained Optimal Control of Distributed Parameter Systems*. Phd thesis, University of Alberta, Edmonton, AB, Canada.
- Christofides, P. D. (2012). *Nonlinear and robust control of PDE systems*. Systems & Control: Foundations & Applications. Springer, New York, NY.
- Curtain, R. and Zwart, H. (2020). *Introduction to infinite-dimensional systems theory: a state-space approach*, volume 71, chapter 3.2: ‘Riesz-spectral operators’, pages 79–108. Springer Nature.
- Khatibi, S., Cassol, G. O., and Dubljevic, S. (2021). Model predictive control of a non-isothermal axial dispersion tubular reactor with recycle. *Computers & Chemical Engineering*, 145:107159.
- Krstić, M. (2009). *Delay compensation for nonlinear, adaptive, and PDE systems*, chapter 1.8: ‘DDE or Transport PDE Representation’, page 9. Systems & control. Birkhäuser.
- Liu, L., Huang, B., and Dubljevic, S. (2014). Model predictive control of axial dispersion chemical reactor. *Journal of Process Control*, 24(11):1671–1690.
- Moadeli, B., Cassol, G. O., and Dubljevic, S. (2025). Optimal control of axial dispersion tubular reactors with recycle: Addressing state-delay through transport PDEs. *The Canadian Journal of Chemical Engineering*, 103(8):3751–3766.

References (cont.)

- Moadeli, B. and Dubljevic, S. (2025a). Advanced control of non-isothermal axial dispersion tubular reactors with recycle-induced state delay. *The Canadian Journal of Chemical Engineering*. Under review.
- Moadeli, B. and Dubljevic, S. (2025b). Model predictive control of axial dispersion tubular reactors with recycle: Addressing state-delay through transport pdes. In *2025 American Control Conference (ACC)*, pages 2323–2328.
- Moadeli, B. and Dubljevic, S. (2025c). Observer-based MPC design of an axial dispersion tubular reactor: Addressing recycle delays through transport PDEs. In *2025 European Control Conference (ECC)*, Thessaloniki, Greece. In Press.
- Xu, Q. and Dubljevic, S. (2017). Linear model predictive control for transport-reaction processes. *AIChE Journal*, 63(7):2644–2659.
- Xu, X. and Dubljevic, S. (2016). The state feedback servo-regulator for countercurrent heat-exchanger system modelled by system of hyperbolic pdes. *European Journal of Control*, 29:51–61.

Appendix A-1: Parameters Used in Isothermal Simulations

Table: Physical Parameters for the Isothermal System

Parameter	Symbol	Value	Unit
Diffusivity	D	2×10^{-5}	m^2/s
Velocity	v	0.01	m/s
Reaction Constant	k_r	-1.5	s^{-1}
Recycle Residence Time	τ	80	s
Recycle Ratio	R	0.3	—

Appendix A-2: Parameters Used in Non-isothermal Simulations

Table: Parameters Used in the Steady-State Analysis for Case I (Unstable) and Case II (Stable) of the Non-isothermal System

Parameter	Case I (Unstable)	Case II (Stable)
Pe_m	4	4
Pe_T	6	6
T_w^{ss}	-0.37	-0.37
T_{Feed}	600 K	600 K
$C_{A,Feed}$	1.0 M	1.0 M
k_a	0.6	0.6
r_r	0.3	0.3
α	0.8	0.8
η	14.0	6.0
σ	0.9	0.9
τ	0.5	0.5
R_1	-1.38	-0.45
R_2	6.48	1.95

Appendix B: Resolvent Derivation (1/3)

Step 1: Apply Laplace transform and reformulate in space

$$\begin{aligned}\dot{x}(\zeta, t) &= Ax(\zeta, t) + Bu(t) \xrightarrow{\mathcal{L}} \\ sX(\zeta, s) - x(\zeta, 0) &= AX(\zeta, s) + BU(s)\end{aligned}\quad (19)$$

Step 2: Convert PDE to spatial ODE in ζ

$$\underbrace{\partial_{\zeta} \begin{bmatrix} X_1 \\ \partial_{\zeta} X_1 \\ X_2 \end{bmatrix}}_{\tilde{X}} = \underbrace{\begin{bmatrix} 0 & 1 & 0 \\ \frac{s-k}{D} & \frac{v}{D} & 0 \\ 0 & 0 & s\tau \end{bmatrix}}_{P(s)} \tilde{X} + \underbrace{\begin{bmatrix} 0 \\ -\frac{x_1(\zeta, 0)}{D} + v(1-R)\delta(\zeta)U(s) \\ -\tau x_2(\zeta, 0) \end{bmatrix}}_{Z(\zeta, s)} \quad (20)$$

Solution (variation of constants):

$$\tilde{X}(\zeta, s) = e^{P(s)\zeta} \tilde{X}(0, s) + \int_0^{\zeta} e^{P(s)(\zeta-\eta)} Z(\eta, s) d\eta \quad (21)$$

Appendix B: Resolvent Derivation (2/3)

Step 3: Solve for $\tilde{X}(0, s)$ using nonhomogeneous boundary conditions

$$\underbrace{\begin{bmatrix} -v & D & Rv \\ T_{11}(1, s) & T_{12}(1, s) & -T_{33}(1, s) \\ T_{21}(1, s) & T_{22}(1, s) & 0 \end{bmatrix}}_{M^{-1}(s)} \tilde{X}(0, s) = \int_0^1 \begin{bmatrix} 0 \\ F_{33}(1, \eta)Z_3 - F_{12}(1, \eta)Z_2 \\ -F_{22}(1, \eta)Z_2 \end{bmatrix} d\eta \quad (22)$$

This gives $\tilde{X}(0, s)$, which is then substituted back into the general solution to form the resolvent operator.

Appendix B: Resolvent Derivation (3/3)

Final expressions for $R(s, A)$

Zero-state (initial condition = 0):

$$R_1 B = -v(1 - R) \left[\sum_{j=1}^2 T_{1j}(\zeta) (M_{j2} T_{12}(1) + M_{j3} T_{22}(1)) - T_{12}(\zeta) \right]$$

$$R_2 B = -v(1 - R) T_{33}(\zeta) (M_{32} T_{12}(1) + M_{33} T_{22}(1))$$

Zero-input (input = 0):

$$R_{11} = \sum_{j=1}^2 \frac{T_{1j}(\zeta)}{D} \int_0^1 [M_{j2} F_{12}(1, \eta) + M_{j3} F_{22}(1, \eta)] (\cdot)_1 d\eta - \frac{1}{D} \int_0^\zeta F_{12}(\zeta, \eta) (\cdot)_1 d\eta$$

$$R_{12} = -\tau \sum_{j=1}^2 T_{1j}(\zeta) \int_0^1 M_{j2} F_{33}(1, \eta) (\cdot)_2 d\eta$$

$$R_{21} = \frac{T_{33}(\zeta)}{D} \int_0^1 [M_{32} F_{12}(1, \eta) + M_{33} F_{22}(1, \eta)] (\cdot)_1 d\eta$$

$$R_{22} = -\tau T_{33}(\zeta) \int_0^1 M_{32} F_{33}(1, \eta) (\cdot)_2 d\eta - \tau \int_0^\zeta F_{33}(\zeta, \eta) (\cdot)_2 d\eta$$